

Magnetic-Field Effect as a Tool to Investigate Electron Correlation in Strong-Field Ionization

Kang Lin^{1,3,*}, Xiang Chen,^{2,4} Sebastian Eckart¹, Hui Jiang,² Alexander Hartung,¹ Daniel Trabert,¹ Kilian Fehre,¹ Jonas Rist¹, Lothar Ph. H. Schmidt,¹ Markus S. Schöffler,¹ Till Jahnke,⁵ Maksim Kunitski,¹ Feng He,^{2,6,†} and Reinhard Dörner^{1,‡}

¹*Institut für Kernphysik, Goethe-Universität Frankfurt am Main, Frankfurt am Main 60438, Germany*

²*Key Laboratory for Laser Plasmas (Ministry of Education) and School of Physics and Astronomy, Collaborative Innovation Center for IFSA (CICIFSA), Shanghai Jiao Tong University, Shanghai 200240, China*

³*State Key Laboratory of Precision Spectroscopy, East China Normal University, Shanghai 200241, China*

⁴*Shanghai Baoshan Science and Technology Committee, Shanghai 200940, China*

⁵*European XFEL, Schenefeld 22869, Germany*

⁶*CAS Center for Excellence in Ultra-intense Laser Science, Shanghai 201800, China*

 (Received 7 January 2022; accepted 25 February 2022; published 16 March 2022)

The influence of the magnetic component of the driving electromagnetic field is often neglected when investigating light-matter interaction. We show that the magnetic component of the light field plays an important role in nonsequential double ionization, which serves as a powerful tool to investigate electron correlation. We investigate the magnetic-field effects in double ionization of xenon atoms driven by near-infrared ultrashort femtosecond laser pulses and find that the mean forward shift of the electron momentum distribution in light-propagation direction agrees well with the classical prediction, where no under-barrier or recollisional nondipole enhancement is observed. By extending classical trajectory Monte Carlo simulations beyond the dipole approximation, we reveal that double ionization proceeds via recollision-induced doubly excited states, followed by subsequent sequential over-barrier field ionization of the two electrons. In agreement with this model, the binding energies do not lead to an additional nondipole forward shift of the electrons. Our findings provide a new method to study electron correlation by exploiting the effect of the magnetic component of the electromagnetic field.

DOI: [10.1103/PhysRevLett.128.113201](https://doi.org/10.1103/PhysRevLett.128.113201)

Electron correlation is a fundamental ingredient in atomic, molecular, and solid-state quantum systems. For atoms and molecules exposed to moderately strong laser fields, nonsequential double ionization (NSDI) is mediated by electron-electron interaction, which gives rise to strong correlations [1,2]. Following the first observation in 1983 by l'Huillier *et al.* [3], many experiments [4–9] confirmed the “knee” structure in the plot of double ionization yield as a function of laser intensity, which cannot be described in any single-active-electron models such as, e.g., the Ammosov-Delone-Krainov (ADK) theory [10]. Under many circumstances, the knee structure is well explained by the semiclassical three-step model [11]. First, a bound electron is released to the continuum by tunneling through the barrier formed by the superposition of the atomic field and the external electric field of the driving laser pulse. Subsequently, the freed electron gains energy from the laser field and is driven back to its parent ion. Finally, the returning electron recollides inelastically with the parent ion to kick out a second correlated electron, leading to the NSDI [12–18]. The magnetic field was believed not to produce noticeable effects because of its much smaller magnitude as compared to the electric component of the

driving electromagnetic field. This is also the reason why many implementations of the three-step model, which accounts only for the electric force, successfully explain the electron correlation in the NSDI over a wide range of laser intensities and wavelengths [19–30], including the quantitative semiclassical model [19], the mechanism of recollision excitation with subsequent ionization [20–22], and the classical description for various NSDI trajectories [23–30].

However, already in 1998, Crawford and Reiss investigated the strong-field ionization beyond the dipole approximation [31]. Recent experimental [32–38] and theoretical [39–44] progress in the understanding of the role of the magnetic field and the retardation of the electric field in strong-field ionization have posed questions to the dipole-approximation-based models of the NSDI. Pioneering theoretical works showed that the effective gate on the initial momentum of the returning electron wave packet is slightly shifted by the magnetic field in the light-propagation direction [45,46]; i.e., only electrons launched with small initial momentum against the light-propagation direction can return close to the parent ion, as the initial momentum is necessary to compensate for the forward shift

induced by the Lorentz force. The magnitude of the forward shift induced by a near-infrared laser field is much smaller than the electron's wave packet initial transverse momentum spread. Moreover, theoretical works on single ionization [47–49] predicted that the freed electron experiences the Lorentz force not only after tunneling but already as it crosses the tunnel, resulting in an additional forward shift of $I_p/(3c)$ in the electron momentum, where I_p is the ionization potential of the atom and c is the speed of light (atomic units are used unless stated otherwise). This prediction has been experimentally tested by tracking the mean value of the electron momentum component in light-propagation direction $\langle p_x \rangle$ for the electron's kinetic energy E_e [50], confirming that

$$\langle p_x \rangle(E_e) = \frac{E_e}{c} + \frac{1}{3} \times \frac{I_p}{c}. \quad (1)$$

Up to now, it has been completely unexplored how this translates to double ionization, where two electrons and two different ionization potentials are involved. A naive assumption for sequential double ionization would be

$$\langle p_{x1} + p_{x2} \rangle(E_{\text{sum}}) = \frac{E_{\text{sum}}}{c} + \frac{1}{3} \times \frac{I_{p1} + I_{p2}}{c}. \quad (2)$$

Here, E_{sum} is the sum kinetic energy of the two electrons, and I_{p1} and I_{p2} represent the first and second ionization potentials of the target atom, respectively. However, the situation becomes nontrivial when it comes to NSDI, where correlation between the two electrons is involved. How will the electron correlation affect the $(I_{p1} + I_{p2})/(3c)$ term in Eq. (2)? In addition to this open question, Emmanouilidou and Meltzer [51] predicted that the sum nondipole shift of the two electrons $\langle p_{x1} + p_{x2} \rangle$ will be greatly enhanced due to the recollision process in the NSDI as compared to twice the one of single ionization. This additional enhancement was recently confirmed by Sun *et al.* for argon atoms using midinfrared laser pulses [52].

In the present Letter, we invert the chain of arguments. Instead of trying to treat the magnetic field as a perturbation that leads to quantitatively small corrections of the observables, we use the magnetic field as a tool to investigate the electron correlation in the NSDI of xenon atoms. Our findings are twofold. First, we find no sum under-barrier nondipole shift that corresponds to $(I_{p1} + I_{p2})/(3c)$ for the two electrons. Our observed nondipole shifts coincide with the classical prediction for free electrons, which is given by

$$\langle p_{x1} + p_{x2} \rangle(E_{\text{sum}}) = \frac{E_{\text{sum}}}{c}. \quad (3)$$

Second, no recollisional enhancement of the nondipole forward shift is found. The observed nondipole shifts for electron pairs emitted to the same and opposite hemispheres are congruent. These findings resolve a long-

standing controversy on which mechanism governs the NSDI in high- Z atoms by adding a magnetic-field-induced nondipole shift as an additional observable. Among the mechanisms proposed to explain the enhanced double ionization in Xe are direct two-electron ejection [3], shake-off processes during tunneling [6], field-independent resonant excitation [8], high-order sequential ionization [53], and a phase-space perspective [54]. Further, a puzzling finding was the lack of correlation between the momenta of the two electrons from double ionization of Xe [55]. This is remarkably different from the typical fingerlike structures [56,57] of low- Z atoms when plotting the momentum component of one electron parallel to the laser polarization versus the respective momentum of the other electron. Our nondipole classical trajectory Monte Carlo (CTMC) simulation reveals that an intermediate doubly excited state is formed after the recollision. In this model, the returning electron is recaptured by the parent ion and simultaneous excitation of a second bound electron allows for the dielectronic recombination [58–60]. Subsequently, the two highly excited electrons are over-barrier ionized in the residual laser field. Our explanation of the NSDI through an intermediate doubly excited state is supported by the aforementioned two pieces of experimental evidence. The new I'_{p1} and I'_{p2} of the excited state are close to zero so that the $(I'_{p1} + I'_{p2})/(3c)$ term vanishes. The recollisional nondipole shift is transferred to the ion during the formation of the doubly excited state.

Experimentally, we adopt the same strategy as described in Refs. [38,50]. The output (25 fs, 800 nm, 10 kHz) of a Ti:sapphire laser system (Coherent Legend Elite Duo) is split into two pathways using a dielectric beam splitter. The intensity and polarization of each laser pathway can be adjusted independently. The two linearly polarized laser beams are focused into the vacuum chamber of a cold target recoil ion momentum spectroscopy (COLTRIMS) reaction microscope [61] from two opposite sides onto the same spot inside a supersonic gas jet of xenon atoms using two independent lenses ($f = 25$ cm). For both laser pulses the polarization axis is aligned along the z direction. Two motorized shutters placed in the two beam pathways are used to toggle between both pathways every 3 min to minimize systematic errors. The peak intensity in the laser focus is found to be 7.0×10^{13} W/cm² with an uncertainty of $\pm 20\%$. For laser intensity calibration, the ratio between the double and the single ionization yield of xenon atoms is recorded and compared to values given in Ref. [7]. A static electric field of 29.8 V/cm was applied to guide the electrons and ions created from double ionization of Xe to two time- and position-sensitive detectors [62] at opposite ends of the spectrometer. The three-dimensional momenta of the electrons and ions were retrieved coincidentally from the times of flight and positions of impact. The z direction is the time-of-flight direction of the COLTRIMS

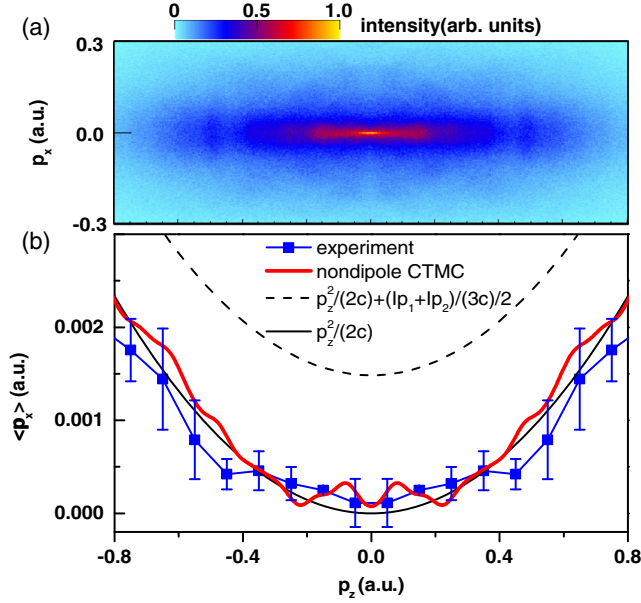


FIG. 1. Experimental results for double ionization of xenon driven by 800 nm, 25 fs laser pulses. (a) Measured two-dimensional electron momentum distribution along the polarization (z axis) and light-propagation (x axis) directions that are measured in coincidence with Xe^{2+} . (b) Mean electron momentum $\langle p_x \rangle$ in the light-propagation direction as a function of p_z along the polarization axis. The error bars show statistical errors.

reaction microscope. The single event electron momentum resolution of our COLTRIMS reaction microscope for the detection of a single electron is 0.003 a.u. in the p_x and p_y directions and 0.03 a.u. in the p_z direction. Owing to the mirror symmetry of the experiment with respect to the light polarization axis (z axis), the data were symmetrized in that dimension.

Figure 1(a) shows the measured two-dimensional electron momentum distribution along the polarization (z axis) and light-propagation (x axis) directions that was coincidentally measured with Xe^{2+} ions. The first and second released electrons are mixed since they are not distinguishable. To visualize the nondipole shift induced by the magnetic field, we calculate the mean electron momentum $\langle p_x \rangle$ for each p_z , where p_z is the electron momentum along the polarization axis, as shown in Fig. 1(b). Strikingly, the mean value $\langle p_x \rangle$ coincides with the classical prediction for a free electron, which is $\langle p_x \rangle = p_z^2/2c$, and no under-barrier nondipole enhancement of $(I_{p1} + I_{p2})/(3c)$ is observed. Practically, here we use the average of the under-barrier nondipole shift of the two electrons for comparison, i.e., $(I_{p1} + I_{p2})/(6c)$, because the temporal order in which the two electrons are released cannot be determined in our experiment as mentioned above. We emphasize that we do not find recollision-induced nondipole enhancement as addressed in simulation and experiment before [51,52].

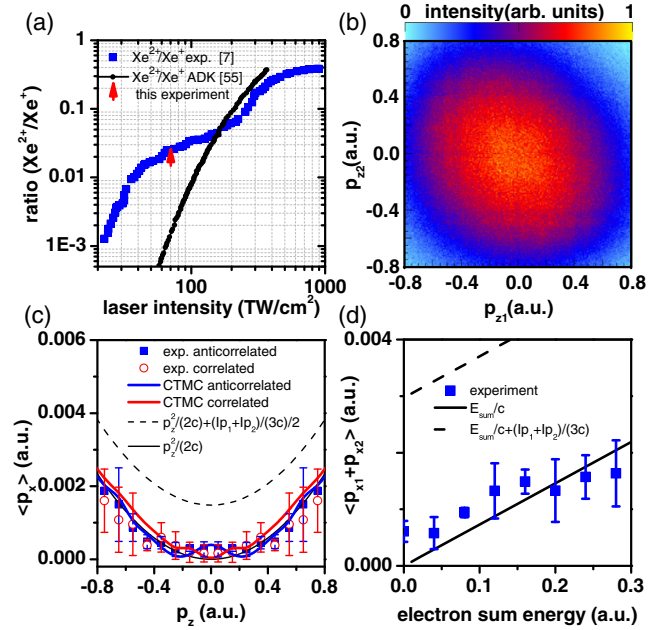


FIG. 2. (a) The ratio between the yields for double and single ionization as a function of the laser intensity for xenon. The blue dotted curve is taken from Ref. [7]. The red arrow indicates the measured ratio and corresponding laser intensity used in our experiment. The black curve is the ratio of $\text{Xe}^{2+}/\text{Xe}^+$ calculated by the ADK model, which is taken from Ref. [55]. (b) The horizontal axis shows the electron momentum component along the polarization axis for one of the two electrons. The vertical axis shows the same momentum component of the other electron. (c) The mean electron momentum $\langle p_x \rangle$ in the light-propagation direction of one of the electrons as a function of its momentum along the polarization axis for correlated [first and third quadrants in (b)] and anticorrelated electron pairs [second and fourth quadrants in (b)]. (d) Mean sum electron momentum $\langle p_{x1} + p_{x2} \rangle$ in the light-propagation direction as a function of the sum kinetic energy of the two electrons. The error bars show statistical errors.

We measure the ratio of $\text{Xe}^{2+}/\text{Xe}^+$ which is presented in Fig. 2(a). It is evident that the measured ratio locates in the knee-structure region, which confirms that the double ionization events are dominated by the nonsequential process. Figure 2(b) shows the measured electron-electron correlation map, i.e., the momentum components of the two electrons along the light polarization axis, which agrees with previous findings for xenon atoms [55]. In this map, events that are located in the first and third quadrants correspond to cases in which both electrons are ejected into the same hemisphere (correlated emission), while for events in the second and fourth quadrants the two electrons are ejected into opposite hemispheres (anticorrelated emission). In the following, we present the nondipole shift curves $\langle p_x \rangle(p_z)$ for the correlated and anticorrelated electron pairs in Fig. 2(c), respectively. It is surprising that the two curves of $\langle p_x \rangle(p_z)$ are congruent and coincide well with the classical prediction for a free electron. Our finding is in contrast to that using the low- Z argon atoms [52],

where the correlated electrons are found to have a larger forward-shifted peak as compared to that of near-axis electrons. The similarity of correlated and anticorrelated electrons further confirms the absence of recollisional nondipole enhancement. To better visualize the contribution from the magnetic field to the electron pair, we plot the mean sum momentum $\langle p_{x1} + p_{x2} \rangle$ with respect to their sum kinetic energy E_{sum} in Fig. 2(d) by selecting events where the two electrons and a Xe^{2+} ion are measured in coincidence. Again, our findings agree well with the classical prediction of $\langle p_{x1} + p_{x2} \rangle = E_{\text{sum}}/c$ and show no additional shift on the order of $(I_{p1} + I_{p2})/(3c)$. This indicates that, even though the energy $(I_{p1} + I_{p2})$ is supplied by the laser field, no fraction of the corresponding photon momentum of $(I_{p1} + I_{p2})/c$ is transferred to the electrons. As a consequence, it can be concluded that this forward momentum must be taken up by the doubly charged ion.

In the following, we discuss the underlying physics by performing nondipole CTMC simulations [46] based on the three-step model [11]. In the first step, we use the ADK model to describe the tunneling process [10]. To artificially account for the magnetic-field effect under the barrier, a forward momentum shift of $I_{p1}/(3c)$ [47–50] along the light-propagation direction is added to the initial transverse momentum distribution of $W(v_x, v_y) = [2(2I_{p1})^{1/2}/|E(\tau)|] \times \exp\{\{[v_x - I_{p1}/(3c)]^2 + v_y^2\}(2I_{p1})^{1/2}/|E(\tau)|\}$, where $I_{p1} = 0.45$ a.u. is the first ionization energy of xenon and $\tau = t - x/c$ is the light cone coordinate. We assume that tunneling is adiabatic and neglect any initial momenta in the direction of tunneling. After tunneling, the subsequent evolution of the electron in the electromagnetic field is modeled using Newton's equation of motion. The dynamics are governed by the expression $(d^2\mathbf{r}/dt^2) = -\nabla_r(V_{ne}^{\text{GSZ}} + V_{ee}) + q\mathbf{E}(\tau) + q\mathbf{v} \times \mathbf{B}(\tau)$, where V_{ne}^{GSZ} represents the Coulomb interaction between a nucleus and an electron, and V_{ee} represents the Coulomb interaction between two electrons. To account for the effect of the inner electrons of high- Z atoms (xenon), the Green-Sellin-Zachor (GSZ) potential formula $V_{ne}^{\text{GSZ}}(r) = \{-[2 + (Z-2)\Omega(r)]/r\}$ is used in our simulation [63–66], where $\Omega(r) = \{1/[(\eta/\xi)(e^{\xi r} - 1) + 1]\}$ with nuclear charge $Z = 54$ and two screening parameters $\eta = 5.2075$ and $\xi = 1.1701$. Here the soft-core parameter $s = 0.1$ is used in $r = \sqrt{x^2 + y^2 + z^2} + s$ to remove the singularity of the potential. Newton's equations of motion are solved by using the Runge-Kutta algorithm. The electric field of the linearly polarized laser pulse is expressed as $\mathbf{E}(\tau) = f(\tau)\mathbf{E}_0 \cos(\omega\tau)\hat{\mathbf{e}}_z$, and the magnetic field is given by $\mathbf{B}(\tau) = \hat{\mathbf{e}}_x \times \mathbf{E}(\tau)/c$, where $f(\tau)$ is the pulse envelope with three-cycle plateau followed by one-cycle ramp off. The second electron is initialized in a bound state using the microcanonical distribution [46,51] with an ionization potential of $I_{p2} = 0.78$ a.u.

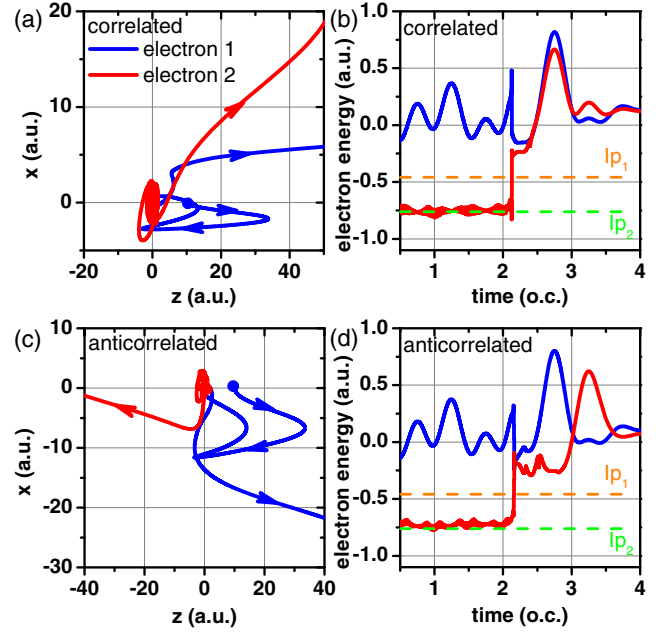


FIG. 3. Nondipole CTMC simulation results. Electron trajectories in real space in the xz plane (x , light-propagation direction; z , polarization axis) for (a) correlated and (c) anticorrelated electrons. The energies of the first and second electrons are shown as a function of time in units of laser cycles (o.c.) for (b) correlated and (d) anticorrelated electrons.

Figures 3(a) and 3(c) show two typical electron trajectories that have correlated and anticorrelated final momenta. The trajectories are shown in the plane formed by the light-propagation and the polarization axes for a double ionization event. For both cases, the most interesting feature of the first electron trajectory is that it circles the ionic core after it is driven back, which indicates the recapture of the rescattering electron by its parent ion and leads to the formation of a highly excited Rydberg state. For better visualization, we plot the time-resolved electron energy in Figs. 3(b) and 3(d). When the first electron circles the ionic core in real space, its energy drops drastically to negative values, accompanied by the excitation of the second bound electron by forming a doubly excited state with close-to-zero binding energy. In the case of the correlated electron pair, the two electrons are both ionized by the remaining laser field within the same half cycle [Fig. 3(b)]. In contrast, for the anticorrelated electron pair, the two electrons are ionized sequentially in different half cycles, and ultimately propagate along opposite directions [Fig. 3(d)]. Since the two electrons are stripped off from a doubly excited state, it is expected that the $(I_{p1} + I_{p2})/(3c)$ offset disappears. Upon its initial release the first electron is launched with a forward shift of $I_{p1}/(3c)$ in the light-propagation direction, however, this amount is transferred to the ionic core during the recapture of the electron. To this end, the total photon momentum offset of I_{p1}/c that corresponds to the energy needed to

overcome the binding potential of the first electron is fully gained by the ionic core.

In conclusion, we show that no under-barrier and no recollisional nondipole enhancement is observed in the NSDI of xenon driven by a near-infrared ultrashort femto-second laser pulse. This allows us to address the physical origin of the remarkably different electron correlation dynamics for high- Z atoms as compared to the one of low- Z atoms. This magnetic-field perspective confirms that a doubly excited state is formed after the first electron recollides with its parent ion, followed by further sequential over-barrier double ionization, which finally eliminates the nondipole contribution from the initial tunneling and recollision step. Our findings pave the way for further investigating the nondipole effect in strong-field driven electron correlation dynamics.

The experimental work was supported by the DFG (German Research Foundation). K. L. acknowledges support by the Alexander von Humboldt Foundation. S. E. acknowledges funding of the DFG through Priority Programme SPP 1840 QUTIF. A. H. and K. F. acknowledge support by the German Academic Scholarship Foundation. F. H. acknowledges the support by the National Science Foundation of China (No. 11925405, No. 91850203). We acknowledge helpful discussions with Fenghao Sun and Hongcheng Ni.

*lin@atom.uni-frankfurt.de

†fhe@sjtu.edu.cn

*doerner@atom.uni-frankfurt.de

- [1] T. Weber, H. Giessen, M. Weckenbrock, G. Urbasch, A. Staudte, L. Spielberger, O. Jagutzki, V. Mergel, M. Vollmer, and R. Dörner, *Nature (London)* **405**, 658 (2000).
- [2] W. Becker, X. J. Liu, P. J. Ho, and J. H. Eberly, *Rev. Mod. Phys.* **84**, 1011 (2012).
- [3] A. l’Huillier, L. A. Lompre, G. Mainfray, and C. Manus, *Phys. Rev. A* **27**, 2503 (1983).
- [4] D. N. Fittinghoff, P. R. Bolton, B. Chang, and K. C. Kulander, *Phys. Rev. Lett.* **69**, 2642 (1992).
- [5] B. Walker, B. Sheehy, L. F. DiMauro, P. Agostini, K. J. Schafer, and K. C. Kulander, *Phys. Rev. Lett.* **73**, 1227 (1994).
- [6] A. Talebpour, C.-Y. Chien, Y. Liang, S. Larochelle, and S. L. Chin, *J. Phys. B* **30**, 1721 (1997).
- [7] J. L. Chaloupka, J. Rudati, R. Lafon, P. Agostini, K. C. Kulander, and L. F. DiMauro, *Phys. Rev. Lett.* **90**, 033002 (2003).
- [8] J. Rudati, J. L. Chaloupka, P. Agostini, K. C. Kulander, and L. F. DiMauro, *Phys. Rev. Lett.* **92**, 203001 (2004).
- [9] A. D. DiChiara, E. Sistrunk, C. I. Blaga, U. B. Szafruga, P. Agostini, and L. F. DiMauro, *Phys. Rev. Lett.* **108**, 033002 (2012).
- [10] M. V. Ammosov, N. B. Delone, and V. P. Krainov, *Sov. Phys. JETP* **64**, 1191 (1986), <http://www.jetp.ras.ru/cgi-bin/e/index/e/64/6/p1191?a=list>.
- [11] P. B. Corkum, *Phys. Rev. Lett.* **71**, 1994 (1993).
- [12] T. Weber, M. Weckenbrock, A. Staudte, L. Spielberger, O. Jagutzki, V. Mergel, F. Afaneh, G. Urbasch, M. Vollmer, H. Giessen, and R. Dörner, *Phys. Rev. Lett.* **84**, 443 (2000).
- [13] R. Moshhammer, B. Feuerstein, W. Schmitt, A. Dorn, C. D. Schröter, J. Ullrich, H. Rottke, C. Trupp, M. Wittmann, G. Korn, K. Hoffmann, and W. Sandner, *Phys. Rev. Lett.* **84**, 447 (2000).
- [14] M. Kübel, K. J. Betsch, N. G. Kling, A. S. Alnaser, J. Schmidt, U. Kleineberg, Y. Deng, I. Ben-Itzhak, G. G. Paulus, T. Pfeifer, J. Ullrich, R. Moshhammer, M. F. Kling, and B. Bergues, *New J. Phys.* **16**, 033008 (2014).
- [15] B. Bergues, M. Kübel, N. G. Johnson, B. Fischer, N. Camus, K. J. Betsch, O. Herrwerth, A. Senfleben, A. M. Sayler, T. Rathje *et al.*, *Nat. Commun.* **3**, 813 (2012).
- [16] G. Gingras, A. Tripathi, and B. Witzel, *Phys. Rev. Lett.* **103**, 173001 (2009).
- [17] Y. Liu, S. Tschuch, A. Rudenko, M. Dürr, M. Siegel, U. Morgner, R. Moshhammer, and J. Ullrich, *Phys. Rev. Lett.* **101**, 053001 (2008).
- [18] Y. Liu, D. Ye, J. Liu, A. Rudenko, S. Tschuch, M. Dürr, M. Siegel, U. Morgner, Q. Gong, R. Moshhammer, and J. Ullrich, *Phys. Rev. Lett.* **104**, 173002 (2010).
- [19] G. L. Yudin and M. Y. Ivanov, *Phys. Rev. A* **63**, 033404 (2001).
- [20] T. Shaaran, M. T. Nygren, and C. Figueira de Morisson Faria, *Phys. Rev. A* **81**, 063413 (2010).
- [21] T. Shaaran, B. B. Augstein, and C. Figueira de Morisson Faria, *Phys. Rev. A* **84**, 013429 (2011).
- [22] C. F. d. M. Faria, T. Shaaran, and M. T. Nygren, *Phys. Rev. A* **86**, 053405 (2012).
- [23] S. L. Haan, P. S. Wheeler, R. Panfili, and J. H. Eberly, *Phys. Rev. A* **66**, 061402(R) (2002).
- [24] R. Panfili, S. L. Haan, and J. H. Eberly, *Phys. Rev. Lett.* **89**, 113001 (2002).
- [25] P. J. Ho and J. H. Eberly, *Phys. Rev. Lett.* **95**, 193002 (2005).
- [26] P. J. Ho, R. Panfili, S. L. Haan, and J. H. Eberly, *Phys. Rev. Lett.* **94**, 093002 (2005).
- [27] S. L. Haan, L. Breen, A. Karim, and J. H. Eberly, *Phys. Rev. Lett.* **97**, 103008 (2006).
- [28] S. L. Haan, Z. S. Smith, K. N. Shomsky, and P. W. Plantinga, *J. Phys. B* **41**, 211002 (2008).
- [29] S. L. Haan, J. S. Van Dyke, and Z. S. Smith, *Phys. Rev. Lett.* **101**, 113001 (2008).
- [30] K. N. Shomsky, Z. S. Smith, and S. L. Haan, *Phys. Rev. A* **79**, 061402(R) (2009).
- [31] D. P. Crawford and H. R. Reiss, *Opt. Express* **2**, 289 (1998).
- [32] C. T. L. Smeenk, L. Arissian, B. Zhou, A. Mysyrowicz, D. M. Villeneuve, A. Staudte, and P. B. Corkum, *Phys. Rev. Lett.* **106**, 193002 (2011).
- [33] A. Ludwig, J. Maurer, B. W. Mayer, C. R. Phillips, L. Gallmann, and U. Keller, *Phys. Rev. Lett.* **113**, 243001 (2014).
- [34] J. Maurer, B. Willenberg, J. Daněk, B. W. Mayer, C. R. Phillips, L. Gallmann, M. Klaiber, K. Z. Hatsagortsyan, C. H. Keitel, and U. Keller, *Phys. Rev. A* **97**, 013404 (2018).
- [35] N. Haram, I. Ivanov, H. Xu, K. T. Kim, A. Atia-tul-Noor, U. S. Sainadh, R. D. Glover, D. Chetty, I. V. Litvinyuk, and R. T. Sang, *Phys. Rev. Lett.* **123**, 093201 (2019).

- [36] B. Willenberg, J. Maurer, U. Keller, J. Daněk, M. Klaiber, N. Teeny, K. Z. Hatsagortsyan, and C. H. Keitel, *Phys. Rev. A* **100**, 033417 (2019).
- [37] B. Willenberg, J. Maurer, B. W. Mayer, and U. Keller, *Nat. Commun.* **10**, 5548 (2019).
- [38] A. Hartung, S. Brennecke, K. Lin, D. Trabert, K. Fehre, J. Rist, M. S. Schöffler, T. Jahnke, L. P. H. Schmidt, M. Kunitski, M. Lein, R. Dörner, and S. Eckart, *Phys. Rev. Lett.* **126**, 053202 (2021).
- [39] M. Klaiber, K. Z. Hatsagortsyan, and C. H. Keitel, *Phys. Rev. A* **71**, 033408 (2005).
- [40] M. Klaiber, K. Z. Hatsagortsyan, and C. H. Keitel, *Phys. Rev. A* **75**, 063413 (2007).
- [41] E. Yakaboylu, M. Klaiber, H. Bauke, K. Z. Hatsagortsyan, and C. H. Keitel, *Phys. Rev. A* **88**, 063421 (2013).
- [42] S. Brennecke and M. Lein, *Phys. Rev. A* **98**, 063414 (2018).
- [43] S. Brennecke and M. Lein, *J. Phys. B* **51**, 094005 (2018).
- [44] H. Ni, S. Brennecke, X. Gao, P.-L. He, S. Donsa, I. Březinová, F. He, J. Wu, M. Lein, X.-M. Tong, and J. Burgdörfer, *Phys. Rev. Lett.* **125**, 073202 (2020).
- [45] A. Emmanouilidou, T. Meltzer, and P. B. Corkum, *J. Phys. B* **50**, 225602 (2017).
- [46] X. Chen, C. Ruiz, F. He, and J. Zhang, *Opt. Express* **28**, 14884 (2020).
- [47] M. Klaiber, E. Yakaboylu, H. Bauke, K. Z. Hatsagortsyan, and C. H. Keitel, *Phys. Rev. Lett.* **110**, 153004 (2013).
- [48] S. Chelkowski, A. D. Bandrauk, and P. B. Corkum, *Phys. Rev. Lett.* **113**, 263005 (2014).
- [49] P.-L. He, D. Lao, and F. He, *Phys. Rev. Lett.* **118**, 163203 (2017).
- [50] A. Hartung, S. Eckart, S. Brennecke, J. Rist, D. Trabert, K. Fehre, M. Richter, H. Sann, S. Zeller, K. Henrichs *et al.*, *Nat. Phys.* **15**, 1222 (2019).
- [51] A. Emmanouilidou and T. Meltzer, *Phys. Rev. A* **95**, 033405 (2017).
- [52] F. Sun, X. Chen, W. Zhang, J. Qiang, H. Li, P. Lu, X. Gong, Q. Ji, K. Lin, H. Li, J. Tong, F. Chen, C. Ruiz, J. Wu, and F. He, *Phys. Rev. A* **101**, 021402(R) (2020).
- [53] B. Walker, E. Mevel, B. Yang, P. Breger, J. P. Chambaret, A. Antonetti, L. F. DiMauro, and P. Agostini, *Phys. Rev. A* **48**, R894 (1993).
- [54] Y. Shao, Z. Yuan, D. Ye, L. Fu, M.-M. Liu, X. Sun, C. Wu, J. Liu, Q. Gong, and Y. Liu, *J. Opt.* **19**, 124004 (2017).
- [55] X. Sun, M. Li, D. Ye, G. Xin, L. Fu, X. Xie, Y. Deng, C. Wu, J. Liu, Q. Gong, and Y. Liu, *Phys. Rev. Lett.* **113**, 103001 (2014).
- [56] A. Rudenko, V. L. B. de Jesus, T. Ergler, K. Zrost, B. Feuerstein, C. D. Schröter, R. Moshhammer, and J. Ullrich, *Phys. Rev. Lett.* **99**, 263003 (2007).
- [57] A. Staudte, C. Ruiz, M. Schöffler, S. Schössler, D. Zeidler, T. Weber, M. Meckel, D. M. Villeneuve, P. B. Corkum, A. Becker, and R. Dörner, *Phys. Rev. Lett.* **99**, 263002 (2007).
- [58] A. Burgess, *Astrophys. J.* **139**, 776 (1964).
- [59] N. Camus, B. Fischer, M. Kremer, V. Sharma, A. Rudenko, B. Bergues, M. Kübel, N. G. Johnson, M. F. Kling, T. Pfeifer, J. Ullrich, and R. Moshhammer, *Phys. Rev. Lett.* **108**, 073003 (2012).
- [60] Y. Liu, L. Fu, D. Ye, J. Liu, M. Li, C. Wu, Q. Gong, R. Moshhammer, and J. Ullrich, *Phys. Rev. Lett.* **112**, 013003 (2014).
- [61] R. Dörner, V. Mergel, O. Jagutzki, L. Spielberger, J. Ullrich, R. Moshhammer, and H. Schmidt-Böcking, *Phys. Rep.* **330**, 95 (2000).
- [62] O. Jagutzki, A. Cerezo, A. Czasch, R. Dörner, M. Hattas, M. Huang, V. Mergel, U. Spillmann, K. Ullmann-Pfleger, T. Weber, H. Schmidt-Böcking, and G. Smith, *IEEE Trans. Nucl. Sci.* **49**, 2477 (2002).
- [63] A. E. S. Green, D. L. Sellin, and A. S. Zachor, *Phys. Rev.* **184**, 1 (1969).
- [64] P. P. Szydlak and A. E. S. Green, *Phys. Rev. A* **9**, 1885 (1974).
- [65] R. H. Garvey, C. H. Jackman, and A. E. S. Green, *Phys. Rev. A* **12**, 1144 (1975).
- [66] Z. Yuan, D. Ye, J. Liu, and L. Fu, *Phys. Rev. A* **93**, 063409 (2016).